Nucl Med Mol Imaging (2016) 50:196–206
DOI 10.1007/s13139-016-0433-x

REVIEW

ISSN (print) 1869-3482
ISSN (online) 1869-3474

Recent Advances in Nuclear Cardiology

Won Woo Lee[1,2]

Received: 12 May 2016 / Accepted: 24 June 2016 / Published online: 13 July 2016

Abstract Nuclear cardiology is one of the major fields of nuclear medicine practice. Myocardial perfusion studies using single-photon emission computed tomography (SPECT) have played a crucial role in the management of coronary artery diseases. Positron emission tomography (PET) has also been considered an important tool for the assessment of myocardial viability and perfusion. However, the recent development of computed tomography (CT)/magnetic resonance imaging (MRI) technologies and growing concerns about the radiation exposure of patients remain serious challenges for nuclear cardiology. In response to these challenges, remarkable achievements and improvements are currently in progress in the field of myocardial perfusion imaging regarding the applicable software and hardware. Additionally, myocardial perfusion positron emission tomography (PET) is receiving increasing attention owing to its unique capability of absolute myocardial blood flow estimation. An F-18-labeled perfusion agent for PET is under clinical trial with promising interim results. The applications of F-18 fluorodeoxyglucose (FDG) and F-18 sodium fluoride (NaF) to cardiovascular diseases have revealed details on the basic pathophysiology of ischemic heart diseases. PET/MRI seems to be particularly promising for nuclear cardiology in the future. Restrictive diseases, such as cardiac sarcoidosis and amyloidosis, are effectively evaluated using a variety of nuclear imaging tools. Considering these advances, the current challenges of nuclear cardiology will become opportunities if more collaborative efforts are devoted to this exciting field of nuclear medicine.

Keywords Cardiology · Single-photon emission computed tomography · Positron emission tomography · Computed tomography · Perfusion · Myocardial infarction

Introduction

Cardiovascular disease has been the leading cause of death in developed and developing countries. Nuclear cardiology is the field of nuclear medicine that studies cardiovascular diseases. Because cardiovascular disease is still one of the main threats to human health and longevity in many countries, nuclear cardiology can contribute to the management of patients with cardiovascular diseases in many ways. For example, myocardial perfusion single-photon emission computed tomography (SPECT) was the prototypical study of nuclear cardiology that contributed to the management of coronary heart diseases and constituted a major portion of nuclear medicine practice [1]. Positron emission tomography (PET) was advocated as a molecular imaging tool for the assessment of myocardial viability and perfusion [2, 3]. However, the number of nuclear cardiology studies has been steadily declining since the 1990s and the application of these studies faces certain challenges [4, 5]. In response to these challenges, nuclear cardiology is also evolving with the use of advanced technology. In this review article, I present the recent SPECT and PET trends in nuclear cardiology in a variety of clinical situations.

✉ Won Woo Lee
wwlee@snu.ac.kr

[1] Department of Nuclear Medicine, Seoul National University Bundang Hospital, Seoul National University College of Medicine, 82, Gumi-ro 173 Beon-gil, Bundang-gu, Seongnam-si, Gyeonggi-do 463-707, Korea

[2] Institute of Radiation Medicine, Medical Research Center, Seoul National University, Seoul, South Korea

Recent Trends of Myocardial Perfusion Imaging

Development of Hardware

Traditional gamma-camera imaging for myocardial perfusion has been conducted using Anger-type gamma cameras, which comprise scintillator detectors [thallium-doped sodium iodide, NaI(Tl)] as the gamma-photon absorber, photomultiplier tubes for electric signal generation, and Anger-logic computer for the mathematical identification of specific signals [6]. Collimators are placed on top of the scintillator detectors to define the direction of incoming gamma rays. Traditional gamma cameras with large field of view are used for cardiac and non-cardiac general nuclear imaging studies. The high demand for nuclear cardiology applications has motivated manufacturers to develop cardiac-dedicated gamma cameras. These include simple small-field-of-view gamma cameras (CardioMD, Philips Healthcare, Cleveland, OH, USA; Optima and Ventri, GE Healthcare, Little Chalfont, UK), upright and semi-reclining gamma camera (C-Cam, Siemens Healthineers, Erlangen Germany), cardiocentric gamma camera (Cardium Digirad, Suwanee, GA, USA), and cardio-focusing collimated gamma camera (IQ-SPECT, Siemens Healthineers). The most recent and advanced cardiac-dedicated gamma cameras are cadmium-zinc-telluride (CZT)-based gamma cameras (D-SPECT, Spectrum Dynamics Medical, Palo Alto, CA, USA; Discovery 530c or NM/CT 570c, GE Healthcare) (Fig. 1). The practical advantages of the CZT gamma camera compared to conventional gamma cameras are a high (up to 10 times higher) sensitivity and a moderately improved (2–3 times) spatial resolution, which are obtainable in a very short acquisition time (i.e., 2 min) (Table 1) [7–11]. The high sensitivity is also attributed to the use of highly sensitive collimators (parallel-hole collimation with short collimator length and wide collimator inlet or cardio-focusing multi-pinhole collimation) in conjunction with the application of a resolution recovery algorithm [7]. The tungsten-based parallel-hole collimators used in the D-SPECT camera (Spectrum Dynamics Medical) have a wide solid angle for gamma photons that is 8 times larger than that of low-energy high-resolution collimators. This indicates that 8 times more gamma photons are allowed to pass through the collimators, increasing the sensitivity to gamma photons. Generally, the use of high-sensitivity collimators leads to poor spatial resolution. However, in the case of CZT gamma cameras, the intrinsic spatial resolution is excellent, allowing the use of highly sensitive collimators. Besides the inherently high sensitivity of CZT detectors to gamma photons, the extrinsic sensitivity of CZT gamma cameras is also enhanced, as a result. Accordingly, a signal-to-noise ratio that is adequate for image generation is obtained in shorter acquisition times (the so-called ultrafast myocardial perfusion imaging) or using a lower-dose radiopharmaceutical injection than in conventional myocardial perfusion SPECT. Additionally, the high energy resolution of CZT detectors could allow dual isotope injection with simultaneous image acquisition. Consequently, an I-123 metaiodobenzylguanidine (MIBG) sympathetic innervation study and a Tc-99m methoxyisobutylisonitrile (MIBI) myocardial perfusion study can be performed simultaneously without any time interval. The absolute quantitation of myocardial blood flow requires an input function assessment. Usually, the count rate of the left ventricular activity, which is used as an input function, exceeds the counting capacity of conventional NaI(Tl) detectors. In the case of CZT detectors, the obtainable count rate is linear up to maximum value and is sufficiently high enough for the input function

Fig. 1 CZT (cadmium-zinc-telluride)-based gamma cameras. **a** D-SPECT (Spectrum Dynamics Medical): overview, one of nine detectors, and a gantry with nine detectors from left to right. (This figure was originally published by Gambhir et al. [7]. Copyright the Society of Nuclear Medicine and Molecular Imaging). **b** Discovery 530c (GE Healthcare) (*left*), NM/CT570c (GE Healthcare) (*right*). (This figure was originally published by Bocher et al. [73] under the terms of the Creative Commons Attribution Noncommercial License. No change was made)

Table 1 CZT-based gamma camera versus conventional scintillator-based gamma camera: CZT is preferred to scintillator [7–11]

	CZT	Scintillator
Count sensitivity	×5 (cardiac), ×10 (point source)	×1
Spatial resolution	4–5 mm (×2–3 better)	10–11 mm
Acquisition time	2–3 min (theoretically), 5–10 min (practically)	10–20 min
Injection dose for Tc-99m agents	2–5 mCi (theoretically), up to 15 mCi (practically)	>10 mCi
Radiation exposure	4–6 mSv	9–20 mSv
Energy resolution	5.7 % (×1.65 better)	9.4 %
Maximum counts rate for input function evaluation	Linear up to maximum	Intrinsically limited by detector dead time
Size	Compact	Bulky

CZT cadmium-zinc-telluride

assessment. By using a segmental model that is specific for the employed radiopharmaceuticals, CZT gamma cameras could assess the myocardial blood flow at stress and rest and, subsequently, the myocardial flow reserve index. However, neither an attenuation correction nor a scatter correction has been applied to the quantitative approach.

On the other hand, traditional NaI(Tl)-based gamma cameras have some advantages over CZT-based ones (Table 2). Recently introduced commercial gamma cameras are accompanied by algorithms that perform the attenuation and scatter corrections in a truly quantitative manner [12]; these algorithms are not yet available for CZT gamma cameras. In the case of CZT gamma cameras, no real projection images are generated. Cardiac-dedicated gamma cameras are not implemented in institutes that perform a low volume of myocardial perfusion SPECT studies. Large-sized patients are difficult to accommodate in CZT gamma cameras. Furthermore, CZT gamma cameras with the cardiac-focused collimator configuration and an L-type gantry may generate unexpected problems for inferior-wall perfusion assessments and for the detection of left anterior descending coronary artery disease [13, 14]. Actually, the clinical experience in the use of CZT gamma cameras is very limited. However, CZT detectors have many physical advantages over scintillators and manufacturers promote CZT gamma cameras in various configurations [15]. Even non-cardiac gamma cameras may be completely replaced by CZT gamma cameras. The future of gamma camera imaging, whether cardiac or non-cardiac, may be determined by the development of CZT technology.

Development of Software

In terms of software development, iterative reconstruction algorithms like the maximum-likelihood expectation maximization (MLEM) or the ordered-subset expectation maximization (OSEM) algorithms are routinely used. Because OSEM involves a faster processing time than MLEM, it has become more prevalent in recent gamma cameras [16]. The use of OSEM provides myocardial perfusion SPECT images with higher image quality than that obtained with conventional filtered-back projection (FBP) reconstruction. In high-count studies using high injected doses, the difference between the two reconstruction methods may not be substantial; however, in low-count studies using lower injected doses, the advantage of OSEM is evident [17]. During the iterative reconstruction process, a variety of diverse correction methods can be applied, such as attenuation correction, scatter correction, resolution recovery, and noise reduction techniques. The attenuation correction and scatter correction methods have been previously reviewed in the literature [18–21].

Table 2 CZT-based gamma camera versus conventional scintillator-based gamma camera: scintillator is preferred to CZT [7–11]

	CZT	Scintillator
Attenuation correction	Qualitative, only one model	Quantitative, recent models
Scatter correction	Qualitative, only one model	Quantitative, recent models
Projection image	No (pseudo image)	Yes
Versatility	Cardiac only	General nuclear studies
Obese patients	Limited space	Not limited
Cardiac-focused collimation	Problematic for diaphragmatic attenuation and sub-diaphragmatic scatter	Only in a few cardio-centric models
Clinical experience	Limited with mostly single-center studies	Highly experienced with many multi-center studies

CZT cadmium-zinc-telluride

The application of resolution recovery methods has been a leap forward for the improvement of SPECT image quality. The resolution recovery algorithm is integrated into the iterative reconstruction process. During the application of the algorithm, the intrinsic detector response (without the collimator), the extrinsic geometric response (with the collimator), the collimator septal penetration, and the collimator septal scatter are modeled (Fig. 2). In a combination of detector, collimator, gamma energy, orbit shape, and distance between patient and detector, each four components are predicted and compensated using the manufacturer's unique algorithm, resulting in improved spatial resolution and less noise [16, 17]. Septal penetration is not a significant factor in myocardial perfusion SPECT that use low-energy radiopharmaceuticals such as Tl-201 or Tc-99m [17]; however, the application of resolution recovery can sometimes arbitrarily increase the number of obtained counts [12].

Nuclear imaging studies are noisier than radiologic studies. The noisy signals have the features of high frequency. The use of a ramp filter during FBP exacerbates the high-frequency signals but the application of a low-pass filter, such as a Butterworth filter, reduces the noise component. Regarding the iterative reconstruction, a greater number of iterations generate more noise components. To suppress the resultant noise, the iteration number is usually limited and post-reconstruction filters are used. The application of these filters may increase the smoothness of the images but can reduce the contrast between the normal and perfusion defects. Noise reduction algorithms have been developed using a variety of mathematic approaches and the application of noise reduction with resolution recovery can improve the spatial resolution and image contrast compared with FBP reconstruction [17]. Actually, noise reduction was the main innovation in a recently developed state-of-the-art gamma camera (X-SPECT, Siemens Healthineers) [22].

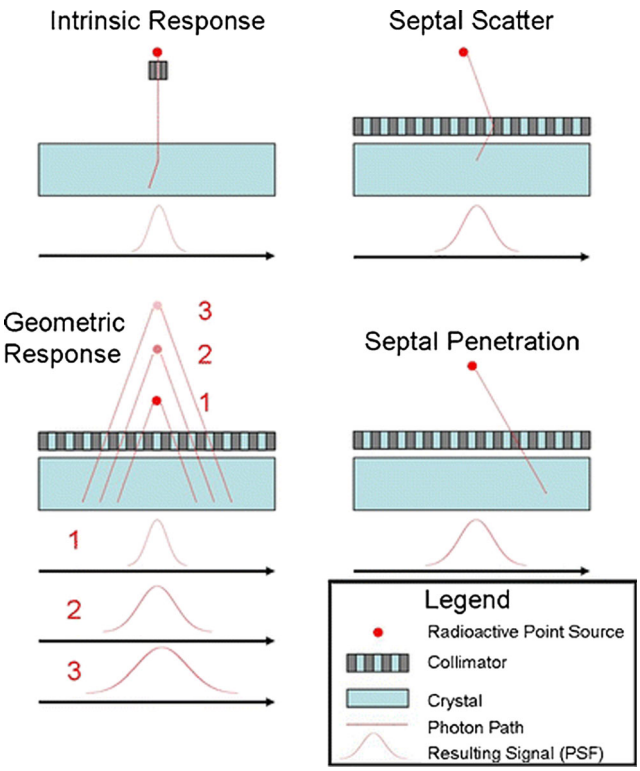

Fig. 2 The components of resolution recovery. (This figure was originally published by Ritt et al. [20] and reused with permission of Springer)

SPECT system manufacturers have developed their own iterative reconstruction algorithms that include resolution recovery and noise reduction functions (Astonish, Philips Healthcare; 3D Flash, Siemens Healthineers; Evolution, GE Healthcare; wide-beam reconstruction, UltraSPECT, Auburndale, MA, USA). CZT gamma cameras also employ these advanced reconstruction software products, further enhancing their image quality [17].

Trends in Myocardial Perfusion Agents

In nuclear cardiology, myocardial perfusion is evaluated using radiopharmaceuticals that have a high first-pass extraction fraction. If a radiopharmaceutical has a perfect first-pass extraction fraction (i.e., microsphere or O-15 H_2O), its uptake degree is not affected by the extraction fraction, but by the blood flow. Consequently, a high extraction fraction is a prerequisite for ideal myocardial perfusion agents. Among the perfusion agents used for gamma camera imaging, Tc-99m teboroxime, Tl-201, Tc-99m MIBI, and Tc-99m tetrofosmin have first-pass extraction fractions of 0.90, 0.85, 0.65, and 0.54, respectively [23]. Conventional gamma cameras using NaI(Tl) scintillators have relatively low sensitivity for gamma photons and typical acquisition times of 10–20 min [9], requiring a sufficiently stable retention of the perfusion agents. Tc-99m MIBI and Tc-99m tetrofosmin become attached to mitochondria of cardiomyocytes and Tl-201 exhibits a redistribution that is sufficiently slow for image acquisition. Therefore, the three above agents have been widely used in NaI(Tl)-based gamma imaging. Recently developed CZT-based gamma cameras have several advantages because of their fast image acquisition. CZT detectors have much higher (5–10 times) sensitivity and moderately improved (2–3 times) spatial resolution compared with scintillator detectors, which enable fast imaging acquisition with durations as short as 2–3 min. Tc-99m teboroxime has been almost ignored as a perfusion agent because its fast kinetics requires a very rapid acquisition (below 5 min) to be performed 2–9 min after injection [17, 24]. Considering the high first-pass extraction of Tc-99m teboroxime, we need to re-think about the use of Tc-99m teboroxime as a perfusion agent for the CZT gamma camera.

Myocardial perfusion PET is more sensitive to coronary heart diseases than myocardial perfusion SPECT [25]. PET

exhibits unparalleled advantages regarding the absolute quantitation of myocardial blood flow and myocardial flow reserve [26]. This quantitative ability of PET originates primarily from the coincidence photon detection [27] and secondarily from the robust algorithms that it employs for the attenuation and scatter corrections, which have yet to be developed for SPECT. The use of CZT-based gamma cameras for the quantitation of myocardial blood flow is currently investigated but no sophisticated attenuation and scatter correction algorithms are available for these systems. Typical perfusion agents used in PET include O-15 H_2O, N-13 NH_3, and Rb-82, which have first-pass extraction fractions 1.0, 0.8–1.0, and 0.5–0.6, respectively [23]. The disadvantage of these PET agents is their relatively short half-lives, particularly for cyclotron-produced O-15 H_2O (2 min) and N-13 NH_3 (10 min). Rb-82 is a generator-produced agent with established diagnostic capability and prognosis predictability [26, 28]. The Sr-82/Rb-82 generator may be imported to Korea in a few years.

Another promising agent for myocardial perfusion PET is F-18 flurpiridaz, which is currently investigated in phase III clinical studies; phase II trial data are already available in the literature (Fig. 3) [29]. F-18 flurpiridaz has been reported to have a high first-pass extraction fraction of 0.9 [30]. Owing to the long half-life of F-18 (110 min) and good pharmacokinetics, F-18 flurpiridaz can be injected during exercise outside the PET scanner room and the image acquisition can be delayed for a certain time. On the other hand, for stress PET studies using other agents (O-15 H_2O, N-13 NH3, and Rb-82), patients must lie on a table inside the PET scanner during the radiopharmaceutical injection. Thus, exercise stress is difficult to test and only pharmacologic stress has been used in traditional myocardial perfusion PET. F-18 flurpiridaz is expected to be marketed in several years.

Challenges in Myocardial Perfusion Imaging

In nuclear cardiology, myocardial perfusion imaging is performed by SPECT and PET, as described above. Myocardial perfusion SPECT has been widely investigated for several decades regarding its diagnostic capability for coronary artery disease. The prognostic value of myocardial perfusion SPECT has also been extensively studied and established and has provided excellent risk stratification for coronary artery disease [31]. However, radiological studies such as cardiac CT and cardiac MRI are competing with nuclear perfusion studies. CT was initially used for coronary calcium accumulation scoring and it progressed to coronary CT angiography and then to myocardial perfusion imaging [32–34]. MRI is useful for the determination of myocardial scar tissue using late-enhancement findings and provides excellent myocardial wall motion and ejection fraction assessments. Nowadays, myocardial perfusion and even coronary angiography are evaluated

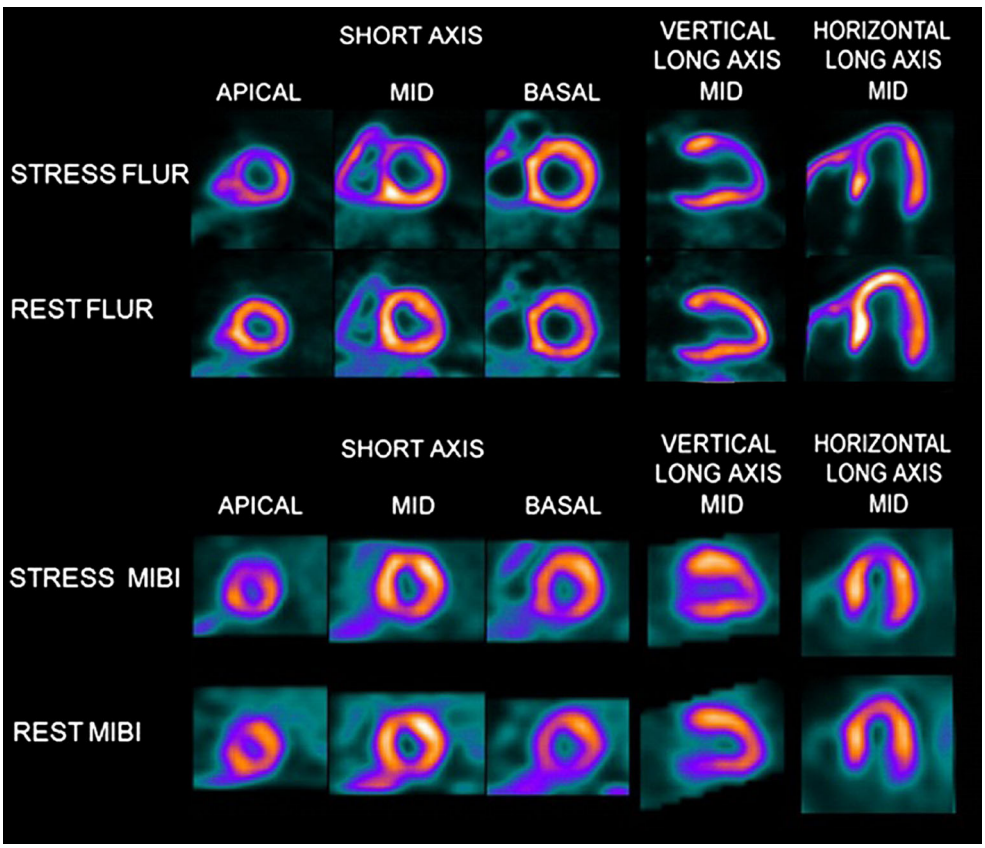

Fig. 3 F-18 flurpiridaz PET versus Tc-99m MIBI SPECT. Reversible perfusion defect in the anterior and antero-septal wall is readily seen in a patient with left anterior descending coronary artery occlusion using F-18 flurpiridaz PET but the perfusion abnormality is not clearly appreciated using Tc-99m MIBI SPECT. (Reprinted from [29] with permission of Elsevier)

using the state-of-the-art MR technology [35–37]. However, anatomical imaging is anatomical imaging, whereas function imaging is functional imaging. The high-resolution imaging achieved by CT and MRI provides excellent anatomical imaging, but SPECT and PET offer the unparalleled advantage of highly sensitive imaging with a true quantitative nature. By combining both imaging modalities, hybrid imaging approaches, such as myocardial perfusion imaging combined with coronary CT angiography (Fig. 4) [38–40] or PET/MRI cardiac imaging [41, 42], have been actively investigated and are expected to become more prevalent in the future.

Another challenge of nuclear cardiology is the high radiation exposure to patients [43]. Radiation exposure from medical imaging studies has been attracting significant attention from the media and the public, and nuclear imaging studies, especially myocardial perfusion SPECT, have been targeted as high-radiation-exposure procedures. In response to this concern, several guidelines have been proposed to reduce unnecessary myocardial perfusion SPECT; these include appropriate use criteria and the optimization of myocardial perfusion SPECT protocols [43]. The American Society of Nuclear Cardiology has suggested the reduction of the overall radiation exposure from myocardial perfusion SPECT in 50 % of the patients to below 9 mSv per study by 2014 [16, 17]. Actually, owing to the development of software and hardware, the radiation exposure of patients was reduced to one-half to one-third of that associated with conventional myocardial perfusion SPECT. In terms of software, the routine use of iterative reconstruction, the application of resolution recovery, and the implementation of noise reduction algorithms are the main factors that have enabled dose reduction without compromising image quality [44]. Regarding hardware development, cardiac-dedicated gamma cameras, especially CZT-based scanners, are the main achievement of this field. Because of their inherently high count sensitivity and spatial resolution compared to conventional NaI(Tl)-based SPECT scanners, the new fast SPECT scanners can complete stress/rest myocardial perfusion SPECT as quickly as within 1 h with a low radiation exposure of 4–6 mSv; this has an especially great clinical impact on younger patients, who are vulnerable to radiation exposure. In these young patients, the acquisition time can be cooperatively increased with reduced injected dose. In the case of older patients, a rapid protocol is preferred because of motion artifact concerns.

Stress-only myocardial perfusion SPECT using Tc-99m agents is a plausible option for low-risk patients without previous myocardial infarction [45, 46]. Stress-only (rest optional) myocardial perfusion SPECT must be accompanied by attenuation corrections and gated wall motion evaluation to increase the diagnostic accuracy. Normal stress study forecasts very low risk of cardiovascular events.

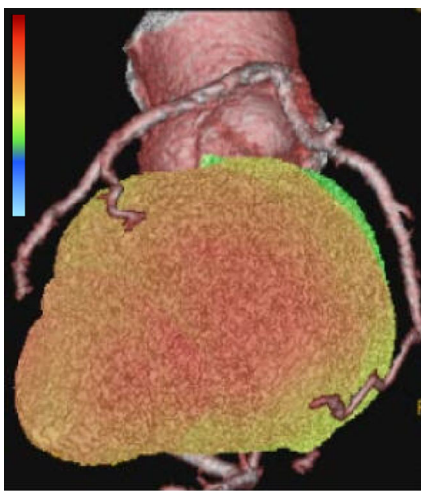

Fig. 4 Three-dimensional fusion of Tc-99m MIBI perfusion SPECT and coronary CT angiography. SPECT image was generated by a dual-head gamma camera (Vertex, ADAC-Philips) and CT angiography image was obtained from in-house PACS system. The fusion process was conducted using CardIQ Fusion software package (GE)

F-18 Fluorodeoxyglucose (FDG) Myocardial PET for Myocardial Infarction

F-18 FDG is widely used in oncology. In nuclear cardiology, F-18 FDG uptake is considered as the biomarker of viable myocardium and a perfusion/metabolism mismatch (i.e., impaired perfusion with increased/preserved metabolism) is characteristic of ischemic viable myocardium that should be rescued through a revascularization procedure [47]. For the detection of viable myocardium, glucose loading with/without intravenous insulin injection is required to enhance F-18 FDG uptake in the normal and the ischemic viable myocardium. The intravenous insulin injection can sometimes induce severe hypoglycemia. Therefore, careful monitoring of the whole-blood glucose level through a finger-stick blood test and the application of a 50 % glucose solution are often required. However, the overall risk to the patients is not high if careful monitoring and timely administration of the glucose solutions are provided to the patients by experienced personnel in the setting of a well-equipped hospital.

Besides traditional viability studies, F-18 FDG uptake in the infarcted myocardium may indicate the presence of post-infarct inflammation (Fig. 5), which is related with the recruitment of inflammatory monocytes to the infarcted tissue [48]. In these circumstances, F-18 FDG uptake in the non-infarcted remote myocardium should be suppressed, in contrast to myocardial viability studies. The inflammation in the infarcted area shows some degree of enhanced F-18 FDG uptake but the F-18 FDG uptake in the infarct is easily surpassed by the surrounding myocardial F-18 FDG uptake. This is similar to cardiac sarcoidosis studies, which require a very complicated protocol for the suppression of F-18 FDG uptake in the normal myocardium. The principal method for F-18 FDG uptake

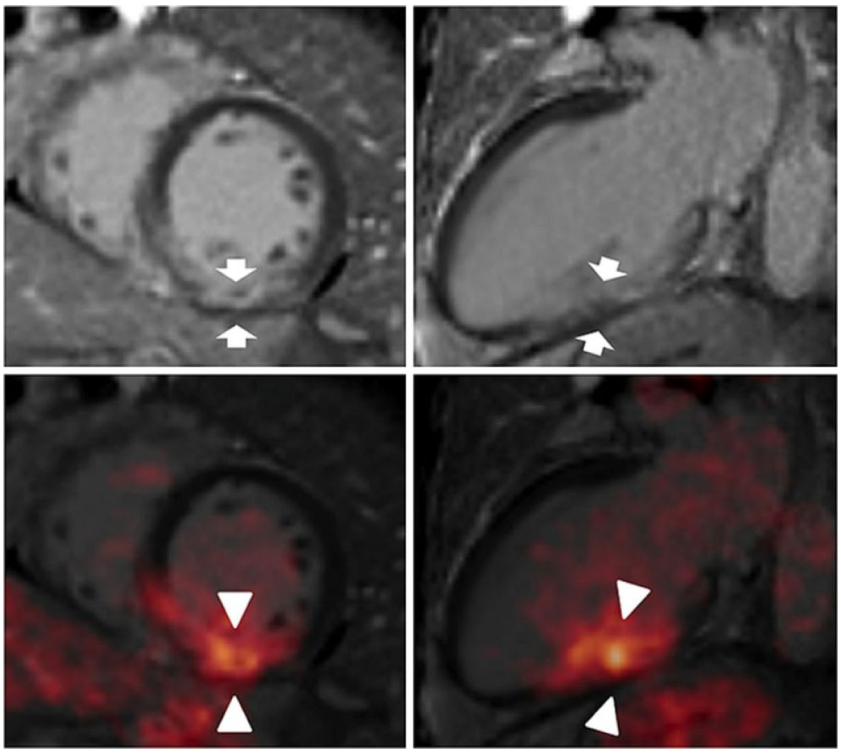

Fig. 5 Increased F-18 FDG uptake in myocardial infarction. Delayed enhancement suggesting subendocardial infarction is shown in the basal inferior wall of MR imaging (*arrows in upper panels*). Increased uptake of F-18 FDG is observed in the same area (*arrowheads in lower panels*). (This research was originally published by Rischpler et al. [74]. Copyright the Society of Nuclear Medicine and Molecular Imaging)

suppression in the normal myocardium entails prolonged (more than 12 h, often up to 18 h) fasting combined with a low-carbohydrate diet. A high-fat diet or unfractionated heparin administration (to increase the free fatty acid level) may also be helpful. Using these complicated protocols, F-18 FDG uptake has been observed in the infarct area at approximately day 5 post-infarction, when the monocyte recruitment reached the peak level. Additionally, the area at risk appeared to have increased F-18 FDG uptake. Interestingly, the increased F-18 FDG uptake in the infarct was related to the poor functional outcome after myocardial infarction [42].

If the typical viability study protocol is applied during the PET study, the degree of F-18 FDG uptake in the infarct area appears to be lower than that in the remote myocardium [41]. The reduced F-18 FDG uptake has been observed in both the infarct area and the area at risk. However, in follow-up PET studies, the reduced F-18 FDG uptake in the area at risk was often normalized [41].

The mentioned F-18 FDG PET studies were conducted using integrated PET/MRI scanners. In addition to oncologic and neurologic applications, cardiac PET/MRI seems to be another promising application of PET/MRI scanners. Late gadolinium enhancement is a well-known phenomenon of myocardial scars and that is successfully used to discriminate transmural and subendocardial infarctions. Furthermore, the recent development of the T2 mapping sequence allows the identification of myocardial edema and is compatible with the area at risk. The relatively slow implementation of PET/MRI in nuclear cardiology involves difficulties of the attenuation correction of PET signals using MR data and the slow development of a PET perfusion agent with long half-life [49]. However, the improvements in these areas are also manifest [50, 51]. Integrated PET/MRI studies could provide an unprecedented opportunity for nuclear cardiology in the near future [41, 42].

F-18 Sodium Fluoride (NaF) PET for Coronary Plaque

F-18 NaF was originally employed as a bone-seeking agent and bone PET using F-18 NaF has been widely used for the evaluation of bone or joint diseases [52–54]. Vascular calcification has been reported to be F-18 NaF-uptake positive, but not all gross calcification observed in CT scans was positive for F-18 NaF uptake [55]. In a recent electron microscopy study, microcalcification was proven to have a greater tendency for F-18 NaF uptake than macrocalcification [56] and F-18 NaF PET is considered to be suitable for the evaluation of early vascular calcification or molecular calcification [57]. Furthermore, high-risk vulnerable plaque appeared to be F-18 NaF-uptake-positive in patients with acute myocardial infarction [58]. The presence of vulnerable plaque is a risk factor for plaque rupture and subsequent acute thrombosis, leading to acute myocardial infarction. F-18 NaF has been reported to be preferable to F-18 FDG for vulnerable plaque imaging because of the lack of background activity from the myocardium [58]. Therefore, the non-invasive identification

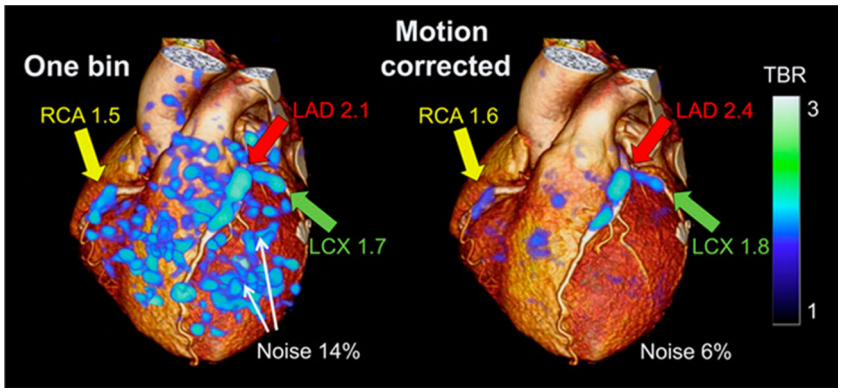

Fig. 6 F-18 NaF PET for coronary atherosclerotic plaques imaging. Application of cardiac motion-frozen algorithm to PET (*right*) reduces noise activity and enables more prominent visualization of coronary plaques, compared to non-corrected PET (*left*). (This research was originally published by Rubeaux et al. [59]. Copyright the Society of Nuclear Medicine and Molecular Imaging)

of such high-risk coronary plaque would have a great clinical impact in the practice of modern cardiology. However, considering the small size of coronary vessels and motion-induced blurring effects in a beating heart, a proper correction for the cardiac and/or respiratory motions is required to ensure the reliable evaluation of the vulnerable plaque (Fig. 6) [59]. In addition, imaging protocols regarding blood activity correction, injected dose, and the use of different PET/CT systems remain to be standardized [60].

Restrictive Heart Disease

The features of restrictive heart disease are a relatively preserved systolic function and the infiltration of cellular or subcellular materials into the myocardium, resulting in the impairment of diastolic relaxation. Imaging studies like echocardiography or cardiac CT/MRI often show only non-specific abnormalities. Among other causative diseases, cardiac sarcoidosis and amyloidosis are the major concerns of nuclear cardiology.

Cardiac sarcoidosis is an inflammatory disease associated with pathologic findings of non-caseating granuloma infiltration to the myocardium [61]. Sarcoidosis is a systemic disease and cardiac involvement of sarcoidosis (i.e., cardiac sarcoidosis) is a risk factor for fatality. Because anti-inflammatory therapy using glucocorticoid is an effective therapeutic option, accurate diagnosis of cardiac sarcoidosis is of paramount importance [62]. Furthermore, the incidence and the prevalence of cardiac sarcoidosis are known to be higher in Asian countries than in Western countries [63]. F-18 FDG PET often shows false-positive uptake in caseating or non-caseating granulomas during oncologic studies, whereas in cardiac sarcoidosis imaging, F-18 FDG PET plays a major role in the

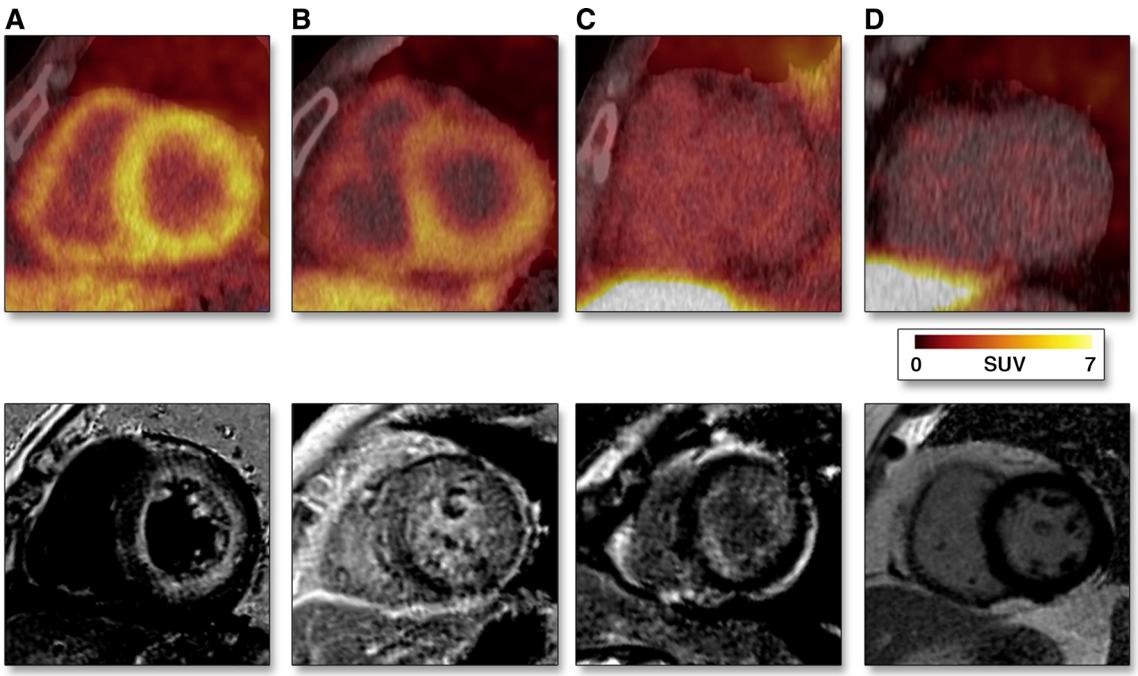

Fig. 7 C-11 PiB PET for light-chain (AL) type amyloidosis. **a** and **b** Chemo-naive AL amyloidosis. **c** Post-therapy AL amyloidosis. **d** Control. (Reprinted from [72] with permission of Elsevier)

evaluation of disease activity [64]. The early classification system for cardiac sarcoidosis did not include F-18 FDG PET, but Ga-67 scans or other gamma-camera imaging studies. However, recently introduced systems adopt F-18 FDG PET as one of the criteria for cardiac sarcoidosis [65]. One of the benefits of F-18 FDG-PET is that the therapeutic response can be effectively evaluated. Furthermore, the F-18 FDG uptake in a heart with perfusion defect findings had prognostic implications [66]. To measure the F-18 FDG uptake in the diseased area, a very complicated preparation is required to suppress the physiologic F-18 FDG uptake in the uninvolved myocardium, as previously described.

Another interesting restrictive heart disease is cardiac amyloidosis. Two types of cardiac amyloidosis exist: transthyretin (TTR) and light-chain (AL). AL-type amyloidosis is known to be a secondary manifestation of a systemic disease of plasma cells. The cardiac involvement of AL amyloidosis is a risk factor for poor prognosis. On the other hand, TTR-type amyloidosis has a relatively milder disease course than AL-type amyloidosis. Regarding the application of nuclear imaging, Tc-99m-labeled phosphates have been used for the imaging of TTR-type amyloidosis. In Europe, Tc-99m 3,3-diphosphono-1,2-propanodicarboxylic acid (DPD) has been widely used, whereas in the US, Tc-99m pyrophosphate has been the preferred imaging agent for this purpose. Tc-99m DPD and Tc-99m pyrophosphate are useful for the differential diagnosis between AL-type amyloidosis (uptake negative) and advanced-stage TTR-type amyloidosis (uptake positive) [67, 68]. Tc-99m methylene diphosphonate (MDP) [69] and Tc-99m hydroxymethylene diphosphonate (HMDP) [70] have also been tested for imaging TTR-type amyloidosis. F-18 NaF, another-bone seeking agent, has been reported to be uptake-positive for TTR-type amyloidosis but negative for AL-type amyloidosis [71]. Alzheimer's disease is characterized by the accumulation of amyloid in brain and several commercial amyloid-targeting PET agents are available. C-11 Pittsburgh B (PiB) was the prototype agent used for brain amyloid imaging. Recently, C-11 PiB PET has been demonstrated to be useful for the evaluation of the cardiac involvement of AL-type amyloidosis (Fig. 7) [72]. In addition to the therapeutic response evaluation, C-11 PiB PET studies have also been used for prognosis prediction.

Conclusions

Nuclear cardiology has been one of the main nuclear medicine practices for several decades. The recent advancements of CT and MR radiologic studies have posed a serious challenge to nuclear cardiology. Radiation exposure is another concern in myocardial perfusion SPECT. However, remarkable achievements have been accomplished in nuclear cardiology in terms of software and hardware. Additionally, the development of novel radiopharmaceuticals will undoubtedly advance nuclear cardiology. Therefore, nuclear cardiology still holds promise as one of the major fields of nuclear medicine.

Compliance with Ethical Standards

Funding This work was supported in part by the Basic Science Research Program through the National Research Foundation of Korea (NRF) funded by the Ministry of Education (2015R1D1A1A01059146) and by Seoul National University Bundang Hospital Research Fund (14-2016-012).

Conflict of Interest Won Woo Lee declares no conflict of interest.

Ethical Approval This work does not contain any studies with human participants or animals.

Informed Consent Not applicable.

References

1. Vitola JV, Shaw LJ, Allam AH, Orellana P, Peix A, Ellmann A, et al. Assessing the need for nuclear cardiology and other advanced cardiac imaging modalities in the developing world. J Nucl Cardiol. 2009;16:956–61.
2. Beanlands RS, Nichol G, Huszti E, Humen D, Racine N, Freeman M, et al. F-18-fluorodeoxyglucose positron emission tomography imaging-assisted management of patients with severe left ventricular dysfunction and suspected coronary disease: a randomized, controlled trial (PARR-2). J Am Coll Cardiol. 2007;50:2002–12.
3. Herzog BA, Husmann L, Valenta I, Gaemperli O, Siegrist PT, Tay FM, et al. Long-term prognostic value of 13N-ammonia myocardial perfusion positron emission tomography added value of coronary flow reserve. J Am Coll Cardiol. 2009;54:150–6.
4. Hendel RC, Berman DS, Di Carli MF, Heidenreich PA, Henkin RE, Pellikka PA, et al. ACCF/ASNC/ACR/AHA/ASE/SCCT/SCMR/SNM 2009 Appropriate Use Criteria for Cardiac Radionuclide Imaging: A Report of the American College of Cardiology Foundation Appropriate Use Criteria Task Force, the American Society of Nuclear Cardiology, the American College of Radiology, the American Heart Association, the American Society of Echocardiography, the Society of Cardiovascular Computed Tomography, the Society for Cardiovascular Magnetic Resonance, and the Society of Nuclear Medicine. J Am Coll Cardiol. 2009;53:2201–29.
5. Rozanski A, Gransar H, Hayes SW, Min J, Friedman JD, Thomson LE, et al. Temporal trends in the frequency of inducible myocardial ischemia during cardiac stress testing: 1991 to 2009. J Am Coll Cardiol. 2013;61:1054–65.
6. Peterson TE, Furenlid LR. SPECT detectors: the Anger Camera and beyond. Phys Med Biol. 2011;56:R145–82.
7. Gambhir SS, Berman DS, Ziffer J, Nagler M, Sandler M, Patton J, et al. A novel high-sensitivity rapid-acquisition single-photon cardiac imaging camera. J Nucl Med. 2009;50:635–43.
8. Garcia EV, Faber TL, Esteves FP. Cardiac dedicated ultrafast SPECT cameras: new designs and clinical implications. J Nucl Med. 2011;52:210–7.
9. Buechel RR, Gaemperli O. Newer generation cameras are preferred. J Nucl Cardiol. 2016; doi:10.1007/s12350-016-0496-1
10. DePuey EG. Traditional gamma cameras are preferred. J Nucl Cardiol. 2016; doi:10.1007/s12350-016-0460-0

11. Henzlova MJ, Duvall WL. Which SPECT for today, which SPECT for tomorrow? J Nucl Cardiol. 2016; doi:10.1007/s12350-016-0496-1
12. Suh MS, Lee WW, Kim YK, Yun PY, Kim SE. Maximum standardized uptake value of Tc hydroxymethylene diphosphonate SPECT/CT for the evaluation of temporomandibular joint disorder. Radiology. 2016; doi:10.1148/radiol.2016152294
13. Kennedy JA, Israel O, Frenkel A. 3D iteratively reconstructed spatial resolution map and sensitivity characterization of a dedicated cardiac SPECT camera. J Nucl Cardiol. 2014;21:443–52.
14. Goto K, Takebayashi H, Yamane H, Hagikura A, Kobayashi K, Morimoto Y, et al. The diagnosis of intermediate coronary artery stenosis by myocardial perfusion imaging using an ultrafast cardiac gamma camera: comparison with fractional flow reserve. Int J Cardiol. 2016;210:66–7.
15. Rhodes DJ, Hruska CB, Phillips SW, Whaley DH, O'Connor MK. Dedicated dual-head gamma imaging for breast cancer screening in women with mammographically dense breasts. Radiology. 2011;258:106–18.
16. Piccinelli M, Garcia EV. Advances in single-photon emission computed tomography hardware and software. Cardiol Clin. 2016;34:1–11.
17. Gordon DePuey 3rd E. Advances in cardiac processing software. Semin Nucl Med. 2014;44:252–73.
18. Hendel RC, Corbett JR, Cullom SJ, DePuey EG, Garcia EV, Bateman TM. The value and practice of attenuation correction for myocardial perfusion SPECT imaging: a joint position statement from the American Society of Nuclear Cardiology and the Society of Nuclear Medicine. J Nucl Cardiol. 2002;9:135–43.
19. Heller GV, Links J, Bateman TM, Ziffer JA, Ficaro E, Cohen MC, et al. American Society of Nuclear Cardiology and Society of Nuclear Medicine joint position statement: attenuation correction of myocardial perfusion SPECT scintigraphy. J Nucl Cardiol. 2004;11:229–30.
20. Ritt P, Vija H, Hornegger J, Kuwert T. Absolute quantification in SPECT. Eur J Nucl Med Mol Imaging. 2011;38 Suppl 1:S69–77.
21. Bailey DL, Willowson KP. An evidence-based review of quantitative SPECT imaging and potential clinical applications. J Nucl Med. 2013;54:83–9.
22. Vija H. Introduction of xSPECT technology: evolving multi-modal SPECT to become context-based and quantitative. Hoffman Estates: Siemens Medical Solutions USA; 2013.
23. Lee DS, Kang WJ, Lee WW, Paeng JC. Cardiovascular system and other circulatory system. In: Chung J-K, Lee M-C, editors. Nuclear Medicine. Seoul: Korea Medical Book Publisher;2008. p. 349–94.
24. Lee JD. Radiopharmaceuticals for myocardial perfusion imaging. In: Lee MC, Chung J-K, editors. Nuclear Cardiology. Seoul: Korea Medical;2002. p. 7–15.
25. Parker MW, Iskandar A, Limone B, Perugini A, Kim H, Jones C, et al. Diagnostic accuracy of cardiac positron emission tomography versus single photon emission computed tomography for coronary artery disease: a bivariate meta-analysis. Circ Cardiovasc Imaging. 2012;5:700–7.
26. Murthy VL, Naya M, Foster CR, Hainer J, Gaber M, Di Carli G, et al. Improved cardiac risk assessment with noninvasive measures of coronary flow reserve. Circulation. 2011;124:2215–24.
27. Bailey DL, Willowson KP. Quantitative SPECT/CT: SPECT joins PET as a quantitative imaging modality. Eur J Nucl Med Mol Imaging. 2014;41 Suppl 1:S17–25.
28. Gould KL, Johnson NP, Bateman TM, Beanlands RS, Bengel FM, Bober R, et al. Anatomic versus physiologic assessment of coronary artery disease. Role of coronary flow reserve, fractional flow reserve, and positron emission tomography imaging in revascularization decision-making. J Am Coll Cardiol. 2013;62:1639–53.
29. Berman DS, Maddahi J, Tamarappoo BK, Czernin J, Taillefer R, Udelson JE, et al. Phase II safety and clinical comparison with single-photon emission computed tomography myocardial perfusion imaging for detection of coronary artery disease: flurpiridaz F 18 positron emission tomography. J Am Coll Cardiol. 2013;61:469–77.
30. Sherif HM, Nekolla SG, Saraste A, Reder S, Yu M, Robinson S, et al. Simplified quantification of myocardial flow reserve with flurpiridaz F 18: validation with microspheres in a pig model. J Nucl Med. 2011;52:617–24.
31. Abidov A, Hachamovitch R, Hayes SW, Friedman JD, Cohen I, Kang X, et al. Are shades of gray prognostically useful in reporting myocardial perfusion single-photon emission computed tomography? Circ Cardiovasc Imaging. 2009;2:290–8.
32. Abdulla J, Abildstrom SZ, Gotzsche O, Christensen E, Kober L, Torp-Pedersen C. 64-multislice detector computed tomography coronary angiography as potential alternative to conventional coronary angiography: a systematic review and meta-analysis. Eur Heart J. 2007;28:3042–50.
33. Hamon M, Morello R, Riddell JW, Hamon M. Coronary arteries: diagnostic performance of 16- versus 64-section spiral CT compared with invasive coronary angiography—meta-analysis. Radiology. 2007;245:720–31.
34. Park JJ, Chun EJ, Cho YS, Oh IY, Yoon CH, Suh JW, et al. Potential predictors of side-branch occlusion in bifurcation lesions after percutaneous coronary intervention: a coronary CT angiography study. Radiology. 2014;271:711–20.
35. Kim RJ, Fieno DS, Parrish TB, Harris K, Chen EL, Simonetti O, et al. Relationship of MRI delayed contrast enhancement to irreversible injury, infarct age, and contractile function. Circulation. 1999;100:1992–2002.
36. Klem I, Heitner JF, Shah DJ, Sketch Jr MH, Behar V, Weinsaft J, et al. Improved detection of coronary artery disease by stress perfusion cardiovascular magnetic resonance with the use of delayed enhancement infarction imaging. J Am Coll Cardiol. 2006;47:1630–8.
37. Cury RC, Shash K, Nagurney JT, Rosito G, Shapiro MD, Nomura CH, et al. Cardiac magnetic resonance with T2-weighted imaging improves detection of patients with acute coronary syndrome in the emergency department. Circulation. 2008;118:837–44.
38. Gaemperli O, Schepis T, Kalff V, Namdar M, Valenta I, Stefani L, et al. Validation of a new cardiac image fusion software for three-dimensional integration of myocardial perfusion SPECT and standalone 64-slice CT angiography. Eur J Nucl Med Mol Imaging. 2007;34:1097–106.
39. Brodov Y, Gransar H, Dey D, Shalev A, Germano G, Friedman JD, et al. Combined quantitative assessment of myocardial perfusion and coronary artery calcium score by hybrid 82Rb PET/CT improves detection of coronary artery disease. J Nucl Med. 2015;56:1345–50.
40. Liga R, Vontobel J, Rovai D, Marinelli M, Caselli C, Pietila M et al. Multicentre multi-device hybrid imaging study of coronary artery disease: results from the EValuation of INtegrated Cardiac Imaging for the Detection and Characterization of Ischaemic Heart Disease (EVINCI) hybrid imaging population. Eur Heart J Cardiovasc Imaging. 2016; doi:10.1093/ehjci/jew038
41. Bulluck H, White SK, Frohlich GM, Casson SG, O'Meara C, Newton A, et al. Quantifying the area at risk in reperfused ST-segment-elevation myocardial infarction patients using hybrid cardiac positron emission tomography-magnetic resonance imaging. Circ Cardiovasc Imaging. 2016;9:e003900.
42. Rischpler C, Dirschinger RJ, Nekolla SG, Kossmann H, Nicolosi S, Hanus F, et al. Prospective evaluation of 18F-Fluorodeoxyglucose uptake in postischemic myocardium by simultaneous positron emission tomography/magnetic resonance imaging as a prognostic marker of functional outcome. Circ Cardiovasc Imaging. 2016;9:e004316.

43. Cerqueira MD, Allman KC, Ficaro EP, Hansen CL, Nichols KJ, Thompson RC, et al. Recommendations for reducing radiation exposure in myocardial perfusion imaging. J Nucl Cardiol. 2010;17:709–18.
44. DePuey EG. Advances in SPECT camera software and hardware: currently available and new on the horizon. J Nucl Cardiol. 2012;19:551–81. quiz 85.
45. Chang SM, Nabi F, Xu J, Raza U, Mahmarian JJ. Normal stress-only versus standard stress/rest myocardial perfusion imaging: similar patient mortality with reduced radiation exposure. J Am Coll Cardiol. 2010;55:221–30.
46. DePuey EG, Ata P, Wray R, Friedman M. Very low-activity stress/high-activity rest, single-day myocardial perfusion SPECT with a conventional sodium iodide camera and wide beam reconstruction processing. J Nucl Cardiol. 2012;19:931–44.
47. D'Egidio G, Nichol G, Williams KA, Guo A, Garrard L, deKemp R, et al. Increasing benefit from revascularization is associated with increasing amounts of myocardial hibernation: a substudy of the PARR-2 trial. JACC Cardiovasc Imaging. 2009;2:1060–8.
48. Lee WW, Marinelli B, van der Laan AM, Sena BF, Gorbatov R, Leuschner F, et al. PET/MRI of inflammation in myocardial infarction. J Am Coll Cardiol. 2012;59:153–63.
49. Kaufmann PA. Cardiac PET/MR: big footprint-small step? J Nucl Cardiol. 2015;22:225–6.
50. Oldan JD, Shah SN, Brunken RC, DiFilippo FP, Obuchowski NA, Bolen MA. Do myocardial PET-MR and PET-CT FDG images provide comparable information? J Nucl Cardiol. 2015; doi:10.1007/s12350-015-0159-7
51. An HJ, Seo S, Kang H, Choi H, Cheon GJ, Kim HJ, et al. MRI-based attenuation correction for PET/MRI using multiphase level-set method. J Nucl Med. 2016;57:587–93.
52. Lee SJ, Lee WW, Kim SE. Bone positron emission tomography with or without CT is more accurate than bone scan for detection of bone metastasis. Korean J Radiol. 2013;14:510–9.
53. Lee H, Lee KS, Lee WW. 18F-NaF PET/CT findings in fibrous dysplasia. Clin Nucl Med. 2015;40:912–4.
54. Lee H, Lee WW, Park SY, Kim SE. F-18 sodium fluoride positron emission tomography/computed tomography for detection of thyroid cancer bone metastasis compared with bone scintigraphy. Korean J Radiol. 2016;17:281–8.
55. Derlin T, Richter U, Bannas P, Begemann P, Buchert R, Mester J, et al. Feasibility of 18F-sodium fluoride PET/CT for imaging of atherosclerotic plaque. J Nucl Med. 2010;51:862–5.
56. Irkle A, Vesey AT, Lewis DY, Skepper JN, Bird JL, Dweck MR, et al. Identifying active vascular microcalcification by (18)F-sodium fluoride positron emission tomography. Nat Commun. 2015;6:7495.
57. Fiz F, Morbelli S, Piccardo A, Bauckneht M, Ferrarazzo G, Pestarino E, et al. ^{18}F-NaF uptake by atherosclerotic plaque on PET/CT imaging: inverse correlation between calcification density and mineral metabolic activity. J Nucl Med. 2015;56:1019–23.
58. Joshi NV, Vesey AT, Williams MC, Shah AS, Calvert PA, Craighead FH, et al. 18F-fluoride positron emission tomography for identification of ruptured and high-risk coronary atherosclerotic plaques: a prospective clinical trial. Lancet. 2014;383:705–13.
59. Rubeaux M, Joshi NV, Dweck MR, Fletcher A, Motwani M, Thomson LE, et al. Motion correction of 18F-NaF PET for imaging coronary atherosclerotic plaques. J Nucl Med. 2016;57:54–9.
60. Blomberg BA, Thomassen A, de Jong PA, Simonsen JA, Lam MG, Nielsen AL, et al. Impact of personal characteristics and technical factors on quantification of sodium 18F-fluoride uptake in human arteries: prospective evaluation of healthy subjects. J Nucl Med. 2015;56:1534–40.
61. Silverman KJ, Hutchins GM, Bulkley BH. Cardiac sarcoid: a clinicopathologic study of 84 unselected patients with systemic sarcoidosis. Circulation. 1978;58:1204–11.
62. Yazaki Y, Isobe M, Hiroe M, Morimoto S, Hiramitsu S, Nakano T, et al. Prognostic determinants of long-term survival in Japanese patients with cardiac sarcoidosis treated with prednisone. Am J Cardiol. 2001;88:1006–10.
63. Bois JP, Chareonthaitawee P. Optimizing radionuclide imaging in the assessment of cardiac sarcoidosis. J Nucl Cardiol. 2016;23:253–5.
64. Youssef G, Leung E, Mylonas I, Nery P, Williams K, Wisenberg G, et al. The use of 18F-FDG PET in the diagnosis of cardiac sarcoidosis: a systematic review and metaanalysis including the Ontario experience. J Nucl Med. 2012;53:241–8.
65. Birnie DH, Sauer WH, Bogun F, Cooper JM, Culver DA, Duvernoy CS, et al. HRS expert consensus statement on the diagnosis and management of arrhythmias associated with cardiac sarcoidosis. Heart Rhythm. 2014;11:1305–23.
66. Blankstein R, Osborne M, Naya M, Waller A, Kim CK, Murthy VL, et al. Cardiac positron emission tomography enhances prognostic assessments of patients with suspected cardiac sarcoidosis. J Am Coll Cardiol. 2014;63:329–36.
67. Rapezzi C, Quarta CC, Guidalotti PL, Longhi S, Pettinato C, Leone O, et al. Usefulness and limitations of 99mTc-3,3-diphosphono-1,2-propanodicarboxylic acid scintigraphy in the aetiological diagnosis of amyloidotic cardiomyopathy. Eur J Nucl Med Mol Imaging. 2011;38:470–8.
68. Bokhari S, Castano A, Pozniakoff T, Deslisle S, Latif F, Maurer MS. (99m)Tc-pyrophosphate scintigraphy for differentiating light-chain cardiac amyloidosis from the transthyretin-related familial and senile cardiac amyloidoses. Circ Cardiovasc Imaging. 2013;6:195–201.
69. Lee VW, Caldarone AG, Falk RH, Rubinow A, Cohen AS. Amyloidosis of heart and liver: comparison of Tc-99m pyrophosphate and Tc-99m methylene diphosphonate for detection. Radiology. 1983;148:239–42.
70. Glaudemans AW, van Rheenen RW, van den Berg MP, Noordzij W, Koole M, Blokzijl H, et al. Bone scintigraphy with (99m)technetium-hydroxymethylene diphosphonate allows early diagnosis of cardiac involvement in patients with transthyretin-derived systemic amyloidosis. Amyloid. 2014;21:35–44.
71. Van Der Gucht A, Galat A, Rosso J, Guellich A, Garot J, Bodez D et al. [18F]-NaF PET/CT imaging in cardiac amyloidosis. J Nucl Cardiol. 2015; doi:10.1007/s12350-015-0287-0
72. Lee SP, Lee ES, Choi H, Im HJ, Koh Y, Lee MH, et al. 11C-Pittsburgh B PET imaging in cardiac amyloidosis. JACC Cardiovasc Imaging. 2015;8:50–9.
73. Bocher M, Blevis IM, Tsukerman L, Shrem Y, Kovalski G, Volokh L. A fast cardiac gamma camera with dynamic SPECT capabilities: design, system validation and future potential. Eur J Nucl Med Mol Imaging. 2010;37:1887–902.
74. Rischpler C, Nekolla SG, Dregely I, Schwaiger M. Hybrid PET/MR imaging of the heart: potential, initial experiences, and future prospects. J Nucl Med. 2013;54:402–15.